

1 **Title: The genome sequence of *Aloe vera* reveals adaptive evolution of drought tolerance**  
2 **mechanisms**

3

4 **Authors:** Shubham K. Jaiswal<sup>1</sup>, Abhisek Chakraborty<sup>1</sup>, Shruti Mahajan<sup>1</sup>, Sudhir Kumar<sup>1</sup>, Vineet K.  
5 Sharma<sup>1\*</sup>

6

7 **Affiliation:**

8 <sup>1</sup>Metagenomics and Systems Biology Group, Department of Biological Sciences, Indian Institute of  
9 Science Education and Research Bhopal

10

11 \*Corresponding Author email:

12 Vineet K. Sharma - vineetks@iiserb.ac.in

13

14 **Email addresses of authors:**

15 Shubham K. Jaiswal - shubhamj@iiserb.ac.in, Abhisek Chakraborty - abhisek18@iiserb.ac.in, Shruti  
16 Mahajan - shruti17@iiserb.ac.in, Sudhir Kumar - sudhir19@iiserb.ac.in, Vineet K. Sharma -  
17 vineetks@iiserb.ac.in

18 **ABSTRACT**

19 *Aloe vera* is a species from Asphodelaceae plant family having unique characteristics such as drought  
20 resistance and also possesses numerous medicinal properties. However, the genetic basis of these  
21 phenotypes is yet unknown, primarily due to the unavailability of its genome sequence. In this study,  
22 we report the first *Aloe vera* draft genome sequence comprising of 13.83 Gbp and harboring 86,177  
23 coding genes. It is also the first genome from the Asphodelaceae plant family and is the largest  
24 angiosperm genome sequenced and assembled till date. Further, we report the first genome-wide  
25 phylogeny of monocots with *Aloe vera* using 1,440 one-to-one orthologs that resolves the genome-  
26 wide phylogenetic position of *Aloe vera* with respect to the other monocots. The comprehensive  
27 comparative analysis of *Aloe vera* genome with the other available high-quality monocot genomes  
28 revealed adaptive evolution in several genes of the drought stress response, CAM pathway, and  
29 circadian rhythm in *Aloe vera*. Further, genes involved in DNA damage response, a key pathway in  
30 several biotic and abiotic stress response mechanisms, were found to be positively selected. This  
31 provides the genetic basis of the evolution of drought stress tolerance capabilities of *Aloe vera*. This  
32 also substantiates the previously suggested notion that the evolution of unique characters in this  
33 species is perhaps due to selection and adaptive evolution rather than the phylogenetic divergence  
34 or isolation.

## 35 INTRODUCTION

36 *Aloe vera* is a succulent and drought-resistant plant belonging to the genus *Aloe* of family  
37 Asphodelaceae [1]. More than 400 species are known in genus *Aloe*, of which four have medicinal  
38 properties with *Aloe vera* being the most potent species [2]. *Aloe vera* is a perennial tropical plant  
39 with succulent and elongated leaves having a transparent mucilaginous tissue consisting of  
40 parenchyma cells in the center referred to as *Aloe vera* gel [3]. The plant is extensively used as a  
41 herb in traditional practices in several countries, and in cosmetics and skin care products due to its  
42 pharmacological properties including anti-inflammatory, anti-tumor, anti-viral, anti-ulcers,  
43 fungicidal, etc. [4, 5]. These medicinal properties emanate from the presence of numerous chemical  
44 constituents such as anthraquinones, vitamins, minerals, enzymes, sterols, amino acids, salicylic  
45 acids, and carbohydrates [6, 7]. These properties make it commercially important, with a global  
46 market worth 1.6 billion [8].

47 One of the key characteristics of this succulent plant is drought resistance that enables it to survive  
48 in adverse hot and dry climates [1]. The plant has thick leaves arranged in an attractive rosette  
49 pattern to the stem. As an adaptation to the hot climate, the plant is able to perform a  
50 photosynthetic pathway known as crassulacean acid metabolism (CAM) that helps in limiting the  
51 water loss by transpiration [9]. Moreover, the leaves have the capacity to store a large volume of  
52 water in their tissues [10]. It is also known to synthesize more of soluble carbohydrates to make the  
53 osmotic adjustments under the limited water conditions, thus improving the water use efficiency  
54 [11]. Though several studies have been performed on drought stress tolerance and potential  
55 benefits of *Aloe vera*, the unavailability of its reference genome sequence has been a deterrent in  
56 understanding the genetic basis and molecular mechanisms of the unique characteristics of this  
57 medicinal plant.

58 In addition to the functional analysis, the resolution of the phylogenetic position has the potential to  
59 reveal the evolutionary history, and to understand the correlations between phylogenetic diversity  
60 and important traits of interest. Multiple attempts have been made to resolve the phylogenetic  
61 position of *Aloe* genus and *Aloe vera*, however, these efforts only used a few conserved loci such as  
62 *rbcl*, *psbA*, *matK*, and ribosomal genes, and could not be performed at genome-wide level due to  
63 the unavailability of the genomic sequence [2, 12, 13]. The previous phylogenies have reported that  
64 *Aloe vera* shared the most common recent ancestor with the species of Poales and Zingiberales  
65 order, also within the Asparagales order, it was closest to the other succulent genera such as  
66 *Haworthia*, *Gasteria*, and *Astroloba* [14, 15].

67 The unavailability of the genome sequence of *Aloe vera* is also noteworthy given the fact that the  
68 representative genomes of species from almost all the plant families, including Brassicaceae,  
69 Cannabaceae, Cucurbitaceae, Euphorbiaceae, Fabaceae, Malvaceae, Rosaceae, Solanaceae, Poaceae,  
70 Orchidaceae, Betulaceae have been sequenced and studied. However, till date, none of the species  
71 from the Asphodelaceae plant family has been sequenced. However, an estimate of the genome size  
72 of *Aloe vera* is available in the Plant DNA c-value database, estimated as 16.04 Gbp with a diploid  
73 ploidy level containing 14 (2n) chromosomes [16]. Thus, the availability of *Aloe vera* genome  
74 sequence will help to reveal the genomic signatures of Asphodelaceae family and will also be useful

75 in understanding the genetic basis of the important phenotypes such as medicinal properties and  
76 drought resistance in *Aloe vera*.

77 Therefore in this study, we report the first draft genome sequence of *Aloe vera* using a hybrid  
78 sequencing and assembly approach by combining the Illumina short-read and oxford nanopore long-  
79 reads sequences to construct the genome sequence. The transcriptome sequencing and analysis of  
80 two tissues, root and leaf, was carried out to gain deep insights into the gene expression and to  
81 precisely determine its gene set. The genome-wide phylogeny of *Aloe vera* with other available  
82 monocot genomes was also constructed to resolve its phylogenetic position. The comparative  
83 analysis of *Aloe vera* with other monocot genomes revealed adaptive evolution in its genes and  
84 provided insights on the stress tolerance capabilities of this species.

85

## 86 **METHODS AND MATERIALS**

### 87 **Sample collection and sequencing**

88 The *Aloe vera* plant was bought from a plant nursery in Bhopal, India. The pulp or gel from the leaf  
89 was scrapped out and the rest was used for the DNA extraction followed by amplification of  
90 complete ITS1 and ITS2 (Internal Transcribed Spacer) and Maturase K (MatK) regions for species  
91 identification. The library was prepared using NEBNext Ultra II DNA Library preparation Kit for  
92 Illumina (New England Biolabs, England) and TruSeq DNA Nano Library preparation kits (Illumina,  
93 Inc., United States). The libraries were sequenced on Illumina HiSeq X ten and NovaSeq 6000  
94 platforms (Illumina, Inc., United States) to generate 150 bp paired-end reads. The DNA extraction for  
95 long read sequencing was performed as per the Oxford nanopore protocols. The purified samples  
96 were used for library preparation by following the protocol of Genomic DNA by Ligation using SQK-  
97 LSK109 kit (Oxford Nanopore, UK). The library was loaded on FLO-MIN106 Flow cell (R 9.4.1) and  
98 sequenced on MinION (Oxford Nanopore, UK) using MinKNOW software (versions 3.4.5 and 3.6.0).  
99 The leaf and root part of plant were used for RNA extraction using TRIzol reagent (Invitrogen, USA).  
100 The library was prepared by using TruSeq Stranded mRNA LT Sample Prep kit and following TruSeq  
101 Stranded mRNA Sample Preparation Guide (Illumina, Inc., United States) and sequenced on Illumina  
102 NovaSeq 6000 platform for 101 bp paired end reads. Prior to sequencing the quality and quantity of  
103 libraries were assessed using Agilent 2100 Bioanalyzer (Agilent Technologies, Santa Clara, CA) and  
104 qPCR, respectively. The detailed methodology and protocols are mentioned in **Supplementary Text**  
105 **S1**.

### 106 **Genome assembly**

107 The raw Illumina sequence data was processed using the Trimmomatic V0.38 tool [17]. For nanopore  
108 data, the adapter sequences were removed by using Porechop v0.2.3. SGA-preqc was used to  
109 estimate the genome size of *Aloe vera* using a k-mer count distribution method [18]. The filtered  
110 paired and unpaired Illumina reads were *de novo* assembled using ABySS v2.1.5 [19]. Different  
111 assemblies were generated on a sample dataset at increasing k-mer values, which showed the best  
112 assembly at k-mer value of 107, and hence the final assembly on complete data was performed at  
113 this k-mer value. The preprocessed nanopore reads were *de novo* assembled using wtdbg2 v2.0.0

114 [20]. The obtained genome assembly was first corrected for the assembly and sequencing errors  
115 using short-read data by SeqBug [21]. The hybrid assembly from the short-read and long-read  
116 assembly was generated by considering only those contigs from the ABySS and wtdbg2 assemblies  
117 that showed less than 50% query coverage and 90% identity using BLASTN against each other. The  
118 RNA-seq data based scaffolding was performed using 'Rascaf', followed by the long-read based gap-  
119 closing performed using LR\_Gapcloser to generate the final *Aloe vera* genome assembly [22]. The  
120 other details about the data preprocessing, genome size estimation, and genome assembly and  
121 polishing are mentioned in **Supplementary Text S2 and Supplementary Figure S1**.

## 122 **Genome annotation**

123 The genome annotation was performed on all the contigs of hybrid assembly. The tandem repeats  
124 were identified using Tandem Repeat Finder (TRF) v4.09 [23]. The microRNAs (miRNAs) were  
125 identified using a homology-based approach using miRBase database, and tRNAs were predicted  
126 using tRNAscan-SE v2.0.5 [24-27] (**Supplementary Text S3**).

## 127 **Transcriptome assembly**

128 The transcriptome assembly of *Aloe vera* was carried out using the RNA-seq data generated from the  
129 root and leaf tissue in this study and previous studies [8, 28]. All the quality-filtered paired and  
130 unpaired transcriptome sequencing reads were *de novo* assembled using Trinity v2.6.6 software with  
131 default parameters to generate the assembled transcripts [29]. The transcriptome assembly was  
132 evaluated by mapping the filtered RNA-seq data on the assembled transcripts using hisat2 v2.1.0  
133 [30]. The BUSCO score was used to assess the completeness of the transcriptome assembly  
134 calculated by BUSCO v4.0.5 software using the standard database specific to the Liliopsida class [31,  
135 32].

## 136 **Gene set construction**

137 The maker pipeline was used for gene set construction of the *Aloe vera* genome [33]. The soft-  
138 masked genome of *Aloe vera* (contigs  $\geq 300$  bp) generated using RepeatMasker v4.1.0 with Repbase  
139 repeat library (RepeatMasker Open-4.0, <http://www.repeatmasker.org>) was used for the gene  
140 prediction using the maker pipeline. Both the *ab initio* and empirical evidence were used for the  
141 gene predictions. The *Aloe vera* EST evidence from the RNA-seq assembly of *Aloe vera* species,  
142 protein sequences of the closest species *Dioscorea rotundata* and *Musa acuminata*, and *ab initio*  
143 gene predictions of the *Aloe vera* genome were used to construct the gene set using the maker  
144 pipeline. AUGUSTUS v3.2.3 was used for the *ab initio* gene prediction, and the BLAST alignment tool  
145 was used for homology-based gene prediction using the EST evidence in the maker pipeline [34-36].  
146 Further, Exonerate v2.2.0 was used to polish and curate the BLAST alignment results  
147 (<https://github.com/nathanweeks/exonerate>). The evidence from *ab initio* and homology-based  
148 methods were integrated to perform the final gene predictions.

149 The genes from predicted transcripts were identified by extracting the longest isoforms. The  
150 unigenes were identified by performing the clustering using CD-HIT-EST v4.8.1 program, and coding  
151 regions were predicted using TransDecoder v5.5.0  
152 (<https://github.com/TransDecoder/TransDecoder>) [37-41]. The gene set constructed using the

153 maker pipeline and transcriptome assembly was filtered, and only the genes with  $\geq 300$  bp length  
154 were considered further. The clustering of remaining maker pipeline based genes was performed  
155 using CD-HIT-EST v4.8.1 program with 95% identity and a seed size of 8 bp [41]. The transcriptome  
156 gene set was searched in the maker gene set using BLASTN. The genes from the transcriptome  
157 assembly gene set that matched to the maker gene set with the parameters: identity  $\geq 50\%$ , e-value  
158  $< 10^{-9}$ , and query coverage  $\geq 50\%$  were removed. The remaining genes for the transcriptome  
159 assembly gene set were directly added to the maker gene set to construct the final gene set of *Aloe*  
160 *vera*.

### 161 **Orthogroups identification**

162 For orthogroups identification, the representative of monocot species from all the clades, for which  
163 high-quality genomes were available on Ensembl plants database, were selected along with an  
164 outgroup species, the model plant *Arabidopsis thaliana*. The selected monocot species were  
165 *Aegilops tauschii*, *Brachypodium distachyon*, *Dioscorea rotundata*, *Eragrostis tef*, *Hordeum vulgare*,  
166 *Leersia perrieri*, *Musa acuminata*, *Oryza sativa*, *Panicum hallii fil2*, *Saccharum spontaneum*, *Setaria*  
167 *italica*, *Sorghum bicolor*, *Triticum aestivum*, and *Zea mays*. The proteome files containing all the  
168 protein sequences of the 15 species retrieved from Ensembl plants release 46 [42], and the protein-  
169 coding genes from the transcriptome assembly of *Aloe vera* were used to construct the orthogroups.  
170 The longest transcript for each gene was extracted for each species using in-house python scripts.  
171 The proteome files with longest transcripts were used for the orthogroups identification using  
172 OrthoFinder v2.3.9 [43]. The OrthoFinder v2.3.9 analysis included a total of 16 species, i.e., 14  
173 monocot species, the model species *Arabidopsis thaliana* as an outgroup, and *Aloe vera* sequenced  
174 in this study.

### 175 **Orthologous gene set construction**

176 From the orthogroups identified by the OrthoFinder analysis, the orthogroups with the taxon count  
177 of 16 were extracted, which included genes from each of the 16 species. A total of 5,472  
178 orthogroups were extracted using this criterion. Only the longest gene of each species was retained  
179 in each of these orthogroups to construct the orthologous gene set. Thus, a total of 5,472 orthologs  
180 were identified across 16 species. From these 5,472 orthologs one-to-one orthologs were extracted.  
181 To include maximum number of genes in the one-to-one orthology, the fuzzy one-to-one  
182 orthogroups instead of true one-to-one orthogroups were identified using KinFin v1.0 [44]. A total of  
183 1,440 one-to-one orthologs were extracted using this method across the selected 16 species.

### 184 **Phylogenetic tree construction**

185 The phylogenetic species tree was constructed with the fuzzy one-to-one orthologous genes. The  
186 individual orthologous sets were aligned using MAFFT v7.455 [45]. The alignments were trimmed  
187 using BeforePhylo v0.9.0 (<https://github.com/qiyunzhu/BeforePhylo>) to remove the poorly aligned  
188 regions. All protein sequence alignments of orthologs across 16 species were concatenated using  
189 BeforePhylo v0.9.0, followed by species phylogenetic tree construction using RAxML v8.2.12 [46].  
190 The maximum likelihood phylogenetic tree was constructed using the rapid hill climbing algorithm

191 with the 100 bootstrap replicates. Since the amino acid sequences were used, the  
192 'PROTGAMMAGTR' substitution model was utilized to construct the species tree.

### 193 **Identification of genes with a higher rate of evolution**

194 The genes that show higher root-to-tip branch length are considered to have a higher rate of  
195 nucleotide divergence or mutation, indicating a higher rate of evolution. For this analysis, the  
196 individual maximum likelihood phylogenetic trees were constructed using the protein sequences of  
197 the 5,472 orthologs identified across the 16 species. The maximum likelihood phylogenetic trees  
198 with 100 bootstrap replicates were constructed using the rapid hill climbing algorithm with the  
199 'PROTGAMMAGTR' substitution model by using RAxML v8.2.12 [46]. The root-to-tip branch length  
200 values were calculated for each of the 16 extant species using the 'adephylo' package in R [47, 48].  
201 All the genes that showed a significantly higher root-to-tip branch length for *Aloe vera* in comparison  
202 to rest of the species were extracted using in-house Perl scripts and were considered to be the genes  
203 with a higher rate of evolution in *Aloe vera*.

### 204 **Identification of positively selected genes**

205 The positively selected genes in *Aloe vera* were identified using the branch-site model implemented  
206 in the PAML software package v4.9a [49]. An iterative program for sequence alignment, SAT'e, was  
207 utilized to perform the alignments of the 5,472 ortholog protein sequences. The combination of  
208 Prank, MUSCLE, and RaxML was used to perform the SAT'e based alignment to control the false  
209 positives and false negatives in the alignment [50]. The protein-alignment guided codon alignment  
210 was performed for the 5,472 ortholog nucleotide sequences using 'TRANALIGN' program of EMBOSS  
211 v6.5.7 package [51]. The 'codeml' was run on ortholog codon alignments using the species  
212 phylogenetic tree constructed in previous steps. The alignments were filtered for the ambiguous  
213 codon sites and gaps and only the clean sites were considered for the positive selection analysis. The  
214 likelihood ratio tests were performed using the log-likelihood values for the null and alternative  
215 models, and the p-values were calculated based on the  $\chi^2$ -distribution. Further, the FDR corrected p-  
216 values or FDR q-values were also calculated. All genes with FDR-corrected p-values <0.05 were  
217 considered to be the genes with positive selection in *Aloe vera*. Further, all codon sites with >0.95  
218 probability of being positively selected in the 'foreground' branch based on the Bayes Empirical  
219 Bayes analysis were considered to be the positively selected codon sites in a gene.

### 220 **Identification of genes with unique substitutions that have functional impact**

221 The genes with unique amino acid substitutions in *Aloe vera* species in comparison to all the selected  
222 species were identified. The protein alignments for the 5,472 orthologs were generated using the  
223 MAFFT v7.455 [45]. The positions that are identical in all the species but different in *Aloe vera* were  
224 identified and considered to be the sites with unique amino acid substitutions in *Aloe vera*. In this  
225 analysis, the gaps were ignored, and also the sites with gaps present in the 10 amino acids flanking  
226 regions on both sides were ignored. This step helped in considering only the sites with proper  
227 alignment for the unique substitution analysis. The identification of unique amino acid sites was  
228 performed by using the in-house python scripts. The functional impact of the unique amino acid



229 substitutions on the protein function was identified using the Sorting Intolerant From Tolerant (SIFT)  
230 tool with UniProt database as reference [52, 53].

### 231 **Identification of genes with multiple signs of adaptive evolution (MSA)**

232 The genes that showed at least two signs of adaptive evolution among the three signs of adaptive  
233 evolution tested above (higher rate of evolution, positive selection, and unique substitution with  
234 functional impact) were considered as the genes with multiple signs of adaptive evolution or MSA  
235 genes in *Aloe vera*.

### 236 **Functional annotation**

237 The functional annotation of gene sets was performed using multiple methods. The functional  
238 annotation and functional categorization of genes into different eggNOG categories was performed  
239 using the eggNOG-mapper [54]. The genes were assigned to different KEGG pathways, and also the  
240 KEGG orthology was determined using the most updated KAAS genome annotation server [55]. The  
241 gene ontology enrichment or GO term enrichment analysis was performed using the WebGestalt  
242 web server [56]. In the over representation analysis, only the GO categories with the p-value <0.05 in  
243 the hypergeometric test were considered to be functionally enriched in the gene set. Further, the  
244 functional annotation of genes was also manually curated. The assignment of genes to the specific  
245 categories and phenotypes was performed by manual annotation. The protein-protein interaction  
246 and co-expression data were extracted from the STRING database, and the network analysis was  
247 performed using Cytoscape [57, 58].

248

## 249 **RESULTS**

### 250 **Sequencing of *Aloe vera* genome and transcriptome**

251 The estimated genome size of *Aloe vera* is 16.04 Gbp, and to comprehensively cover this large  
252 genome, a total of 506.4 Gbp (~32X) of short-reads and 123.5 Gbp (~7.7X) of long-reads data was  
253 generated using Illumina and nanopore platforms, respectively (**Supplementary Table S1 and S2**)  
254 [16, 59]. For transcriptome, a total of 6.6 Gbp and 7.3 Gbp of RNA-seq data was generated from leaf  
255 and root, respectively. The transcriptome data from this study and the publicly available RNA-seq  
256 data from previous studies [8, 28] were combined together, resulting in a total of 37.1 Gbp of RNA-  
257 seq data for *Aloe vera*, which was used for the analysis (**Supplementary Table S3**). All the genomic  
258 and RNA-seq read data were trimmed and filtered using Trimmomatic, and only the high-quality  
259 read data was used to construct the final genome and transcriptome assemblies. The complete  
260 workflow of the sequence analysis is shown in **Supplementary Figure S1**.

### 261 **Assembly of *Aloe vera* genome**

262 The final draft genome assembly of *Aloe vera* had the size of 13.83 Gbp with N50 and largest scaffold  
263 of 3.18 kbp and 4.94 Mbp, respectively (**Supplementary Table S4**). Of which, 12.25 Gbp had length  
264 >300bp with N50 of 7.03 kbp, and 9.85 Gbp had length >500bp with N50 of 13.06 kbp, which is a  
265 challenging feat for such a gigantic plant genome, and is also comparable to the other large plant  
266 genomes assembled till date [60-63]. This was achieved by the hybrid assembly of short-read and



267 long-read data, which was further polished by correction using SeqBug, RNA-seq based scaffolding  
268 using Rascaf, and long-read based gapclosing using LR-gapcloser. The k-mer count distribution-based  
269 method using only the short Illumina reads estimated a genome size of 13.63 Gb, which was smaller  
270 than the c-value-based genome size estimation of 16.04 Gbp, conceivably due to the usage of only  
271 short reads data for the genome size estimation (**Supplementary Figure S2**). The %GC for the final  
272 assembly was 41.98%. The analysis of repetitive sequences revealed 557,638,058 bp of tandem  
273 repeats corresponding to 3.41% of the complete genome.

#### 274 **Transcriptome assembly**

275 The Trinity assembly of transcriptomic reads resulted in a total size of 163,190,792 bp with an N50  
276 value of 1,268 bp and an average contig length of 796 bp (**Supplementary Table S5**). The mapping of  
277 filtered RNA-seq reads on the Trinity transcripts using hisat2 resulted in the overall percentage  
278 mapping of 92.49%. The complete BUSCO score (addition of single copy and duplicates) on the  
279 transcripts was 87.7%. A total of 205,029 transcripts were predicted, corresponding to 108,133  
280 genes with the percent GC of 43.69. The clustering of gene sequences using CD-HIT-EST to remove  
281 the redundancy resulted in 107,672 unigenes. The coding genes (CDS) from the unigenes were  
282 predicted using TransDecoder resulting in 34,269 coding genes.

#### 283 **Genome annotation and gene set construction**

284 A total of 1,978 standard amino acid specific tRNAs and 378 hairpin miRNAs were identified in the  
285 *Aloe vera* genome (**Supplementary Table S6**). The maker pipeline-based gene prediction resulted in  
286 a total of 114,971 coding transcripts, of which 63,408 transcripts ( $\geq 300$  bp) were considered further  
287 for clustering at 95% identity resulting in 57,449 unique coding gene transcripts. Application of the  
288 same length-based selection criteria ( $\geq 300$  bp) on trinity-identified 34,269 coding gene transcripts  
289 resulted in 33,998 coding gene transcripts. The merging to these two coding gene transcript sets  
290 resulted in the final gene set of 86,177 genes for *Aloe vera*, which had the complete BUSCO score of  
291 69.0% and single copy BUSCO score of 65.7%.

#### 292 **Identification of orthologous across selected plant species**

293 A total of 104,543 orthogroups were identified using OrthoFinder across the selected 16 plant  
294 species, of which 9,343 orthogroups were unique to *Aloe vera* and contained genes only from *Aloe*  
295 *vera*. Only a total of 5,472 orthogroups had sequences from all the 16 plant species and were used  
296 for the identification of orthologs. For these 5,472 orthogroups, in case of presence of more than  
297 one gene from a species in an orthogroup, the longest gene representative from that species was  
298 selected to construct the final orthologous gene set for any orthogroups. Thus, including one gene  
299 from each of the 16 species in an orthogroup, a total of 5472 orthologs were identified. In addition,  
300 the fuzzy one-to-one orthologs finding approach applied using KinFin resulted in a total of 1,440  
301 fuzzy one-to-one orthologs that were used for constructing the maximum likelihood species  
302 phylogenetic tree.

### 303 **Resolving the phylogenetic position of *Aloe vera***

304 Each of the 1,440 fuzzy one-to-one orthologous gene set was aligned and concatenated, and the  
305 resulted concatenated alignment had a total of 1,453,617 alignment positions. The concatenated  
306 alignment was filtered for the undetermined values, which were treated as missing values, and a  
307 total of 1,157,550 alignment positions were retained. The complete alignment data and the filtered  
308 alignment data were both used to construct maximum likelihood species trees using RAxML with the  
309 bootstrap value of 100, and both the alignment data resulted in the same phylogeny. Thus, the  
310 phylogeny based on the filtered data was considered to be the final genome-wide phylogeny of *Aloe*  
311 *vera* with all the representative monocot genomes available on Ensembl plants database and  
312 *Arabidopsis thaliana* as an outgroup (**Figure 1**). This phylogeny also corroborated with the earlier  
313 reported phylogenies by Silvera et al., 2014, Dunemann et al., 2014, and Wang et al., 2016, which  
314 were constructed using a limited number of genetic loci [64-66]. It is apparent from the phylogeny  
315 that *Dioscorea rotundata* and *Musa acuminata* are the most closely related to *Aloe vera*, and share  
316 the same clade (**Figure 1**). All other selected monocots are distributed in separate clade with  
317 *Triticum aestivum* and *Aegilops tauschii* being the most distantly related to *Aloe vera*.

318 Recently an updated plant megaphylogeny has been reported for the vascular plants [14]. The  
319 species of Poales order showed similar relative positions in our reported phylogeny and this  
320 megaphylogeny. In the megaphylogeny, *Musa acuminata* was reported to share the most common  
321 recent ancestor with the species of Poales order, but in our phylogeny we observed that *Musa*  
322 *acuminata* shared the most common recent ancestor with *Dioscorea rotundata* from Dioscoreales  
323 order (**Figure 1 and Supplementary Figure S3**). Also, among the selected monocots, the species of  
324 Dioscoreales order was reported to show the earliest divergence. However, in our genome-wide  
325 phylogeny, *Aloe vera* showed the earliest divergence.

326 Also, with respect to the reported phylogeny of angiosperms, at the order level the Poales and  
327 Zingiberales formed a clade, and their ancestor shared the most recent common ancestor with  
328 Asparagales, then all three shared a recent ancestor with Dioscoreales [15]. In our genome-wide  
329 phylogeny, Zingiberales and Dioscoreales shared the most recent common ancestor, and their  
330 ancestor shares the most recent common ancestor with Asparagales, and the three shared a recent  
331 ancestor with Poales.

### 332 **Genes with a higher rate of evolution**

333 A total of 85 genes showed higher rates of evolution in *Aloe vera* in comparison to the other  
334 monocot species. These genes belonged to several eggNOG categories and KEGG pathways, as  
335 mentioned in **Supplementary Table S7 and Supplementary Table S8**, with a higher representation of  
336 ribosomal genes. The distribution of enriched ( $p$ -value $<0.05$ ) biological process GO terms is  
337 mentioned in **Supplementary Table S9**. Also, among these 85 genes, three molecular function GO  
338 terms, rRNA binding, structural constituent of cytoskeleton, and structural constituent of ribosome  
339 showed an enrichment ( $p$ -value $<0.05$ ) (**Supplementary Table S10**). Five transcription factors WRKY,  
340 MYB, bHLH, CPP, and LBD showed higher rates of evolution in *Aloe vera*. Among these, WRKY, MYB,  
341 and bHLH are known to be involved in drought stress tolerance [67-69]. There were six chloroplast

342 functioning related genes, namely EMB3127, PnsB3, TL29, IRT3, PDV2, and SIRB, that showed a  
343 higher rate of evolution. Notably, the chloroplast function related genes have been implicated in  
344 different abiotic stress conditions in plants, including drought [70, 71].

#### 345 **Identification of positively selected genes**

346 A total of 199 genes showed positive selection in *Aloe vera* with the FDR q-value threshold of 0.05.  
347 The distribution of these genes in eggNOG categories, KEGG pathways, and GO term categories are  
348 mentioned in **Supplementary Table S11-S15**. Among the genes with positive selection, several genes  
349 were involved in key functions with specific phenotypic consequences (**Figure 2**). These included  
350 flowering related genes that are important for the reproductive success, calcium-ion binding and  
351 transcription factors/sequence-specific DNA binding genes involved in signal transduction for  
352 response to external stimulus, carbohydrate catabolism genes required for energy production, and  
353 genes involved in abiotic stress response [72-74]. Among the abiotic stress response genes, there  
354 were four categories of genes that were involved in response to water-related stress, DNA damage  
355 response genes involved in reactive oxidative species (ROS) stress response, nuclear pore complex  
356 genes involved in plant stress response by regulating the nucleo-cytoplasmic trafficking, and  
357 secondary metabolites biosynthesis related genes that deal with different types of biotic and abiotic  
358 stresses [75-77]. The robust and efficient DNA damage response mechanism is essential for biotic  
359 and abiotic stress tolerance, and for the genomic stability [78]. Thus, adaptive evolution in this  
360 pathway seemingly contributes towards the stress tolerance capabilities and genomic stability in  
361 *Aloe vera*.

362 Another gene G6PD5 that showed positive selection in *Aloe vera* protects plants against different  
363 types of stress, such as salinity stress by producing nitric oxide (NO) molecule, which leads to the  
364 expression of Defence response genes [79, 80]. Regulation of osmotic potential under drought stress  
365 is acquired by different ion channels, transporters, and carrier proteins [81]. In this study, K<sup>+</sup>  
366 transporter 1(KT1), bidirectional amino acid transporter 1(BAT1), and Sodium Bile acid symporter  
367 (AT4G22840) genes were found to be positively selected in *Aloe vera*.

368 The Abscisic acid (ABA) responsive element binding factor (ABF) gene was found to be positively  
369 selected. This gene is differentially expressed under drought and other abiotic stress and alters  
370 specific target gene expression by binding to ABRE (abscisic acid-response element), the  
371 characteristic element of ABA-inducible genes [82]. ABA also regulates stomatal closure and solute  
372 transport, and thus have implications in drought tolerance [83]. The trehalase 1 (TRE1) gene was  
373 also found to be positively selected, and the over-expression of this gene causes better drought  
374 tolerance through ABA guided stomatal closure [84].

#### 375 **Genes with site-specific signs of evolution**

376 Two types of site-specific signatures of adaptive evolution i.e., positively selected codon sites and  
377 unique amino acid substitutions with significant functional impact were identified in *Aloe vera*. A  
378 total of 1,848 genes had positively selected codon sites, and a total of 2,669 genes had unique amino  
379 acid substitutions with functional impact. The distribution of genes with positively selected codon

380 sites and unique amino acid substitutions with functional impact in eggNOG categories, KEGG  
381 pathways, and GO term categories are mentioned in **Supplementary Tables S16-S25**.

382 One of the characteristics of succulent plants such as *Aloe vera* is the ability to efficiently assimilate  
383 the atmospheric CO<sub>2</sub> and reduce water loss by transpiration through the crassulacean acid  
384 metabolism (CAM) pathway a specific mode of photosynthesis. The evolution of CAM is an  
385 adaptation to the limited CO<sub>2</sub> and limited water condition, and a significant correlation between  
386 higher succulence and increased magnitude of CAM metabolism has been observed [85]. In this  
387 study, several crucial genes of CAM metabolism showed site-specific signatures of adaptive  
388 evolution in *Aloe vera* (**Figure 3**). The potassium channel involved in stomatal opening/closure  
389 (KAT2), malic enzyme (ME) that converts malic acid to pyruvate, and phosphoenolpyruvate  
390 carboxylase (PEPC) that converts phosphoenolpyruvate to oxaloacetate and assimilates the  
391 environmental CO<sub>2</sub> showed both the signs of site-specific adaptive evolution. In addition, the other  
392 CAM genes including potassium transport 2/3 (KT2/3), pyruvate orthophosphate dikinase (PPDK),  
393 phosphoenolpyruvate carboxylase kinase 1 (PPCK1), carbonic anhydrase 1 (CA1), peroxisomal NAD-  
394 malate dehydrogenase 2 (PMDH2), tonoplast dicarboxylate transporter (TDT), and aluminum  
395 activated malate transporter family protein (ALMT9) showed unique substitutions with functional  
396 impact in *Aloe vera*.

397 CAM metabolism evolution is known to be a result of modified circadian regulation at the  
398 transcription and posttranscriptional levels [86]. CAM evolution is the well-characterized  
399 physiological rhythm in plants, and it is also a specific example of circadian clock-based specialization  
400 [86, 87]. Several plant circadian rhythm genes showed site-specific signs of adaptive evolution in  
401 *Aloe vera* (**Figure 4**). Three essential genes of red light response, PHYB, ELF3, and LHY, showed both  
402 the signs of site-specific adaptive evolution. Also, the FT gene important for flowering and under the  
403 control of circadian rhythm showed both the signs of site-specific adaptive evolution. The PHYA  
404 gene, which is also a part of the red light response, had unique substitutions with functional impact.  
405 Among the blue light response genes, three genes GI, FKF1, and SPA2 had unique substitutions with  
406 functional impact, and two genes HY5 and CHS had positively selected codon acid sites. The blue  
407 light response regulates the UV-protection and photomorphogenesis.

408 Plant hormone signaling regulates plant growth, development, and response to different types of  
409 biotic and abiotic stress [88]. Multiple genes of auxin, cytokinin, and brassinosteroid hormone  
410 signaling involved in cellular growth and elongation having implications in cellular and tissue  
411 succulence, showed site-specific signatures of adaptive evolution (**Figure 5**). The genes of the  
412 abscisic acid hormone signaling involved in stomatal opening/closure required for CAM metabolism  
413 and different biotic and abiotic stress response [82] had positively selected amino acid sites and  
414 unique substitution sites with functional impact (**Figure 5**). Also, the genes involved in salicylic acid  
415 signaling important for providing disease resistance and help in biotic stress response showed site-  
416 specific signatures of adaptive evolution (**Figure 5**).

## 417 **Genes with multiple signs of adaptive evolution**

418 Among the three signatures of adaptive evolution i.e., positive selection, a higher rate of evolution,  
419 and unique amino acid substitutions with functional impact, a total of 148 genes showed two or  
420 more signs of adaptive evolution and were identified as the genes with multiple signs of adaptive  
421 evolution (MSA). The distribution of these genes in eggNOG categories, KEGG pathways, and GO  
422 categories are mentioned in **Supplementary Table S26-S29**. Another study that performed the  
423 proteomic analysis of drought stress response in wild peach also found similar categories to be  
424 enriched in the proteins that were differentially expressed under drought conditions [89]. A total of  
425 112 genes out of the 148 MSA genes in *Aloe vera* were from the specific categories that are involved  
426 in providing drought stress tolerance. The specific groups of proteins and their relation with the  
427 drought stress tolerance are mentioned in **Figure 6**.

428 Several ribosomal genes, translational regulators, and transcription factors genes were found to be  
429 MSA genes in this study, and these were also found to be over-expressed under drought conditions  
430 in different proteomic and transcriptomic studies and aid in better drought stress survival [89, 90].  
431 Many nuclear genes are involved in the functioning of symbiotic organelles chloroplast and  
432 mitochondria. Among these genes, some genes are also involved in the organellar gene expression  
433 (OGEs) regulation, and mutants of these genes are known to show altered response to different  
434 abiotic stress, including high salinity stress [91, 92]. Several of these genes belonging to two  
435 categories, RNA helicases and PPR domain proteins, were found to be MSA genes. Thus, in the *Aloe*  
436 *vera* species, these genes have been adaptively evolved to provide this species with better salt  
437 tolerance.

438 Two osmotic biosensor genes, 'CPA' and 'AT2G42100', were found to be among the MSA genes in  
439 *Aloe vera*. Different membrane transporters that can transport signaling molecules, osmolytes, and  
440 metals were also among the MSA genes (**Figure 6**). These included two peroxisomal transporters  
441 'PNC1' a nucleotide carrier protein, and 'PEX14' a transporter for PTS1 and PTS2 domain containing  
442 signaling proteins, different heavy metal transporters such as 'IRT3' an iron transporter,  
443 'AT5G23760' a copper transporter, and 'NRAMP1' a manganese transporter, and 'AT4G17650' a lipid  
444 transporter, 'AT2G40420' an amino acid transporter, 'AT5G06120' an intracellular protein  
445 transporter, 'ALA1' a phospholipid transporter, 'NAT8' a Nucleobase-ascorbate transporter, 'NRT2.6'  
446 a high-affinity nitrate transporter, and 'BASS6' a sodium/metabolite co-transporter. These osmotic  
447 sensors and transporters provide significant enhancement in function in drought stress condition  
448 and help in adjusting to the water scarcity [93, 94].

449 The genes for several kinases and WD-40 repeat proteins were also found to be among the MSA  
450 genes in *Aloe vera*. These proteins are involved in signaling and transcription regulation required for  
451 the drought stress tolerance [90, 95-97]. Also, the genes involved in energy generation and are part  
452 of the thylakoid membrane showed MSA. The stability of thylakoid membrane proteins has been  
453 associated with drought resistance, and these energy production related genes are crucial in survival  
454 during the drought stress [90, 98]. Two genes that assist in protein folding were found to show MSA  
455 (**Figure 6**), and these proteins are very important in protecting the macromolecules of the cells  
456 under the drought stress conditions [99]. Five genes involved in plant hormone signaling were also

457 among the MSA genes. The plant hormone signaling is central to the signaling pathways required for  
458 the drought stress tolerance [100]. Five genes involved in flowering and reproduction regulation  
459 were also found to be among the MSA genes in *Aloe vera*. The flowering and reproduction related  
460 genes are known to be regulated for better reproductive success under drought stress conditions as  
461 part of the drought tolerance strategy used by many plants [101, 102].

462 The co-expression of MSA genes was examined using the co-expression data from the STRING  
463 database [57], and the MSA genes that co-express with at least one other MSA gene are displayed as  
464 a network diagram (**Figure 7A**). From the network, it is evident that almost all co-expressing MSA  
465 genes are drought stress tolerance related, and the genes forming the dense network are also  
466 drought stress tolerance related. Predominantly, three categories of drought stress tolerance related  
467 MSA genes have shown co-expression: genes involved in energy production, genes involved in OGEs  
468 regulation, and genes that predispose plants to drought stress tolerance.

469 Similarly, a network diagram was constructed using the protein-protein interaction data of MSA  
470 genes from the STRING database [57]. The genes with physical interaction known from the  
471 experimental studies are shown in **Figure 7B**. From the network, it is apparent that among the  
472 interacting MSA genes, all of them except one are involved in drought stress tolerance. Further,  
473 among the MSA genes involved in drought stress tolerance, it is primarily the genes that predispose  
474 plants to drought stress tolerance, and the genes involved in signal transduction in drought stress  
475 response showed the physical interaction. In addition, two genes that function as osmotic  
476 biosensors and two OGEs regulation genes also displayed physical interaction.

477

## 478 **DISCUSSION**

479 In this work, we have presented the complete draft genome sequence of *Aloe vera*, which is an  
480 evolutionarily important, ornamental, and widely used plant species due to its medicinal properties,  
481 pharmacological applications, traditional usage, and commercial value. The availability of *Aloe vera*  
482 genome sequence is also important since it is the first genome sequenced from the Asphodelaceae  
483 plant family, and is the largest angiosperm and the fifth largest genome sequenced so far. It is also  
484 the largest genome sequenced using the oxford nanopore technology till date. The hybrid approach  
485 of using short-read (Illumina) and long-read (nanopore) sequence data emerged as a successful  
486 strategy to tackle the challenge of sequencing one of the largest plant genomes.

487 The study reported the gene set of *Aloe vera* constructed using the combination of *de novo* and  
488 homology-based gene predictions, and also using the data from the genomic assembly and the  
489 transcriptomic assembly from multiple tissues, thus indicating the comprehensiveness of the  
490 approach. The *Aloe vera* had a higher number of coding genes than the other monocots used in this  
491 study except for *Triticum aestivum*, which had more number of coding genes (**Supplementary Table**  
492 **S30**). The estimation of coding genes in *Aloe vera* was similar to the number of genes in other  
493 monocot genomes suggesting the correctness of the gene prediction and estimation.

494 This study reported the first genome-wide phylogeny of *Aloe vera* with all other monocot species  
495 available on the Ensembl plant database, and with *Arabidopsis thaliana* as an outgroup. A few



496 previous studies have also examined the phylogenetic position of *Aloe vera* with respect to other  
497 monocots but used a few genomic loci. Thus, this is the first genome-wide phylogeny of monocots  
498 that resolves the phylogenetic position of *Aloe vera* with respect to the other monocots by using  
499 1,440 different loci distributed throughout their genomes. The very high bootstrap values for the  
500 internal nodes and existence of no polytomy in the phylogeny further attest to the correctness of  
501 the phylogeny. This phylogeny is mostly in agreement with the previously known phylogenies, and  
502 also provided some new insights [2, 14, 64-66].

503 An earlier phylogeny constructed using “ppc-aL1a” gene showed that *Sorghum bicolor*, *Zea mays*,  
504 *Setaria italica*, *Brachypodium distachyon*, *Hordeum vulgare*, and *Oryza sativa* form a monophyletic  
505 group, which was also observed in our phylogeny [66]. Similarly, the relative positions of *Hordeum*  
506 *vulgare*, *Saccharum officinarum*, *Zea mays*, and *Oryza sativa* in another phylogeny based on  
507 “CENH3” gene were in agreement with our phylogeny [64]. Using the “NORK” gene, another recent  
508 study reported the relative phylogenetic position of four monocot species: *Oryza sativa*, *Zea mays*,  
509 *Sorghum bicolor*, and *Setaria italica* [65]. *Zea mays*, *Sorghum bicolor*, and *Setaria italica* were  
510 found to share a recent last common ancestor and *Oryza sativa* had diverged earlier from their  
511 common ancestor, which is also supported by the genome-wide phylogeny reported in this study.

512 Though the genome-wide phylogeny showed the species of Poales order with similar topology as  
513 reported in earlier studies, a different topology was observed for the relative position of *Musa*  
514 *acuminata*, *Dioscorea rotundata*, and *Aloe vera* from the orders Zingiberales, Dioscoreales, and  
515 Asparagales, respectively [14, 15]. The observed differences could be due to the usage of a few  
516 genomic loci in the previous phylogenies, whereas the phylogeny reported in this study is a genome-  
517 wide phylogeny constructed using 1,440 one-to-one orthologs distributed across the genome. The  
518 availability of more complete genomes from monocots and the inclusion of more genomic loci in the  
519 phylogenetic analysis will help explain the observed differences and confirm the relative positions of  
520 these species.

521 One of the key highlights of the study was the revelation of adaptive evolution of genes involved in  
522 drought stress response, which provides a genetic explanation for the drought stress tolerance  
523 properties of *Aloe vera*. This plant is known to display a number of phenotypes such as perennial  
524 succulent leaves and CAM mechanism for carbon fixation that provide it with better drought stress  
525 survival [10]. Several experimental studies have also reported that it can make adjustments such as  
526 increased production of sugars and increased expression of heat-shock and ubiquitin proteins for  
527 efficient water utilization and osmotic maintenance that eventually provide better drought survival  
528 [11, 103, 104]. In this study, the majority (80%) of genes that showed multiple signs of evolution  
529 (MSA) were involved in drought stress tolerance related functions. These genes were also found to  
530 be co-expressing and physically interacting with each other, which further point towards the  
531 adaptive evolution of the drought stress tolerance mechanisms in this species. The adaptive  
532 evolution of genes involved in drought stress tolerance provides insights into the genetic basis of the  
533 drought resistance property of *Aloe vera*.

534 Further, several crucial genes of the CAM pathway and circadian rhythm have also shown site-  
535 specific signs of adaptive evolution in *Aloe vera* in comparison to the other monocot species. The



536 CAM pathway has very high water use efficiency, and is known to have evolved convergently in  
537 many arid regions for better drought survival [105]. Also, the CAM pathway is a physiological rhythm  
538 with temporal separation of atmospheric CO<sub>2</sub> assimilation and Calvin-Benson cycle, and is under the  
539 control of plant circadian rhythm [86, 106]. This CAM pathway evolution is known to be a specific  
540 type of circadian rhythm specialization [87, 107]. Thus, the observed adaptive evolution of CAM  
541 pathway and its controller circadian rhythm in this study point towards its role in providing this  
542 species an evolutionary advantage for efficient drought stress survival.

543 The evolutionary success of the *Aloe* genus is also known to be due to the succulent leaf Mesophyll  
544 tissue [2]. Particularly, the medicinal use of *Aloe vera* is much associated with the succulent leaf  
545 mesophyll tissue, and a loss of this tissue leads to the loss of medicinal properties [3]. The plant  
546 species with CAM pathway have large vacuoles in comparison to the non-CAM plants, and therefore  
547 the leaf succulence is also higher in CAM plants. Thus, it is tempting to speculate that the observed  
548 evolution of CAM pathway in *Aloe vera* may also be crucial for the higher leaf mesophyll succulence  
549 contributing to its medicinal properties. Also previously, it has been proposed that the specific  
550 properties of *Aloe vera* such as the high leaf succulence, medicinal properties, and drought  
551 resistance are the consequence of evolutionary processes such as selection and speciation rather  
552 than due to phylogenetic diversity or isolation [2]. The signatures of adaptive evolution in drought  
553 tolerance and CAM pathway genes in *Aloe vera* further substantiate this notion.

554

## 555 **CONCLUSION**

556 The first draft genome, transcriptome, gene set, and functional analysis of *Aloe vera* reported in this  
557 study will act as a reference for future studies to understand the medicinal or evolutionary  
558 characteristics of this species, and its family Asphodelaceae. The first genome-wide phylogeny of  
559 *Aloe vera* and other available monocot genomes resolved the phylogenetic position of *Aloe vera* and  
560 emphasized the need for the availability of more genomes for precise phylogenetic analysis. The  
561 comparative genomic analyses of *Aloe vera* with the other monocot genomes provided novel  
562 insights on the adaptive evolution of drought stress response, CAM pathway, and circadian rhythm  
563 genes in *Aloe vera*, and suggest that the positive selection and adaptive evolution of specific genes  
564 contribute to the unique phenotypes of this species.

565

## 566 **LIST OF ABBREVIATIONS**

567	MSA	Multiple signs of adaptive evolution
568	CAM	Crassulacean acid metabolism
569	COG	Clusters of Orthologous Groups
570	KEGG	Kyoto Encyclopedia of Genes and Genomes
571	GO	Gene ontology
572	BUSCO	Benchmarking Universal Single-Copy Orthologs
573	SIFT	Sorting Intolerant From Tolerant
574	FDR	False discovery rate

575	BLAST	Basic Local Alignment Search Tool
576	N50	minimum contig length needed to cover 50% of the genome
577	ABA	Abscisic acid
578	snoRNA	small nucleolar RNA
579	snRNA	small nuclear RNA
580	tRNA	transfer RNA
581	rRNA	ribosomal RNA
582	srpRNA	signal recognition particle RNA
583	miRNA	micro RNA
584	MYB	Myeloblastosis
585	bHLH	basic helix–loop– helix
586	CPP	cysteine-rich polycomb-like protein
587	LBD	Lateral Organ Boundaries (LOB) Domain
588	EMB3127	Embryo Defective 3127
589	PnsB3	Photosynthetic NDH subcomplex B 3
590	TL29	Thylakoid Lumen 29
591	IRT3	Iron regulated transporter 3
592	PDV2	Plastid Division2
593	SIRB	Sirohydrochlorin ferrochelataase B
594	G6PD5	Glucose-6-phosphate dehydrogenase 5
595	KAT2	Potassium channel in <i>Arabidopsis thaliana</i> 2
596	PHYB	Phytochrome B
597	ELF3	Early Flowering 3
598	LHY	Late Elongated Hypocotyl
599	FT	Flowering locus T
600	PHYA	Phytochrome A
601	GI	Gigantea
602	FKF1	Flavin-binding, Kelch repeat, F box 1
603	SPA1	Suppressor of PHYA-105 1
604	HY5	Elongated Hypocotyl5
605	CHS	Chalcone synthase
606	CPA	Capping Protein A
607	PNC1	Peroxisomal adenine nucleotide carrier 1
608	PEX14	Peroxin 14
609	IRT3	Iron regulated transporter 3
610	NRAMP1	Natural Resistance-Associated Macrophage Protein 1
611	ALA1	Aminophospholipid ATPase 1
612	NAT8	Nucleobase-Ascorbate Transporter 8
613	NRT2.6	High affinity Nitrate Transporter 2.6
614	ppc-aL1a	Phosphoenolpyruvate carboxylase
615	CENH3	Centromeric histone H3

616	NORK	Nodulation receptor kinase
617	PPR	Pentatricopeptide Repeat
618	PTS1	Peroxisomal targeting signal 1
619	PTS2	Peroxisomal targeting signal 2
620	LTR-RT	Long terminal repeat Retrotransposons
621	EST	Expressed sequence tag

622  
623

#### 624 **COMPETING INTERESTS**

625 The authors declare no competing financial and non-financial interest.

626

#### 627 **AUTHORS' CONTRIBUTIONS**

628 VKS conceived and coordinated the project. SM prepared the DNA and RNA samples, performed  
629 sequencing, and the species identification assay. SKJ with the input from VKS designed the  
630 computational framework of the study. SKJ and AC performed the genome assembly, transcriptome  
631 assembly, genome annotation, gene set construction, orthology analysis, and species phylogenetic  
632 tree construction. SKJ performed the root-to-tip branch length, positive selection, unique  
633 substitution with functional impact, network, and statistical analysis. SKJ, AC, SK, and SM performed  
634 the functional annotation of gene sets. SKJ, AC, and VKS analysed the data. SKJ, AC, and VKS  
635 interpreted the results. SKJ and AC constructed the figures. SKJ, AC, SM, SK, and VKS wrote and  
636 revised the manuscript. All the authors have read and approved the final version of the manuscript.

637

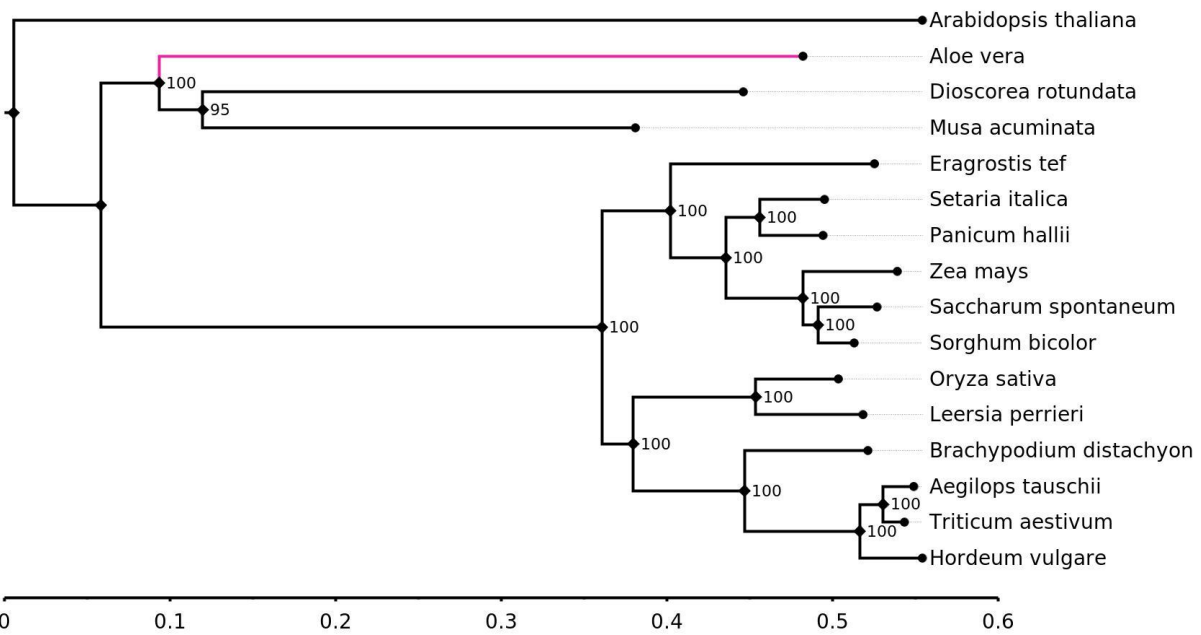
#### 638 **ACKNOWLEDGEMENTS**

639 The author SKJ thanks Department of Science and Technology for the DST-INSPIRE fellowship. AC  
640 and SM thank Council of Scientific and Industrial Research (CSIR) for fellowship. SK thanks University  
641 Grants Commission (UGC) for the fellowship. We also thank the intramural research funds provided  
642 by IISER Bhopal.

643

644

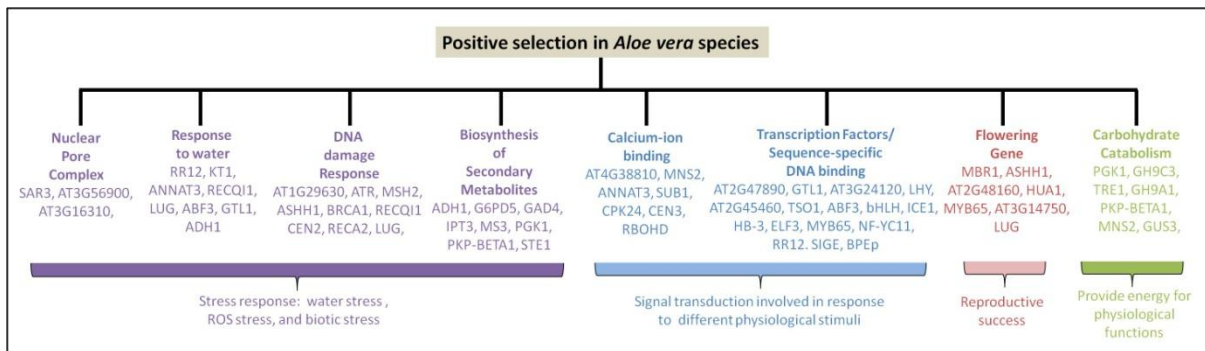
645 **FIGURES**



646  
647 **Figure 1.** The phylogenetic tree of the selected 14 monocot species, *Aloe vera*, and *Arabidopsis*  
648 *thaliana* as an outgroup

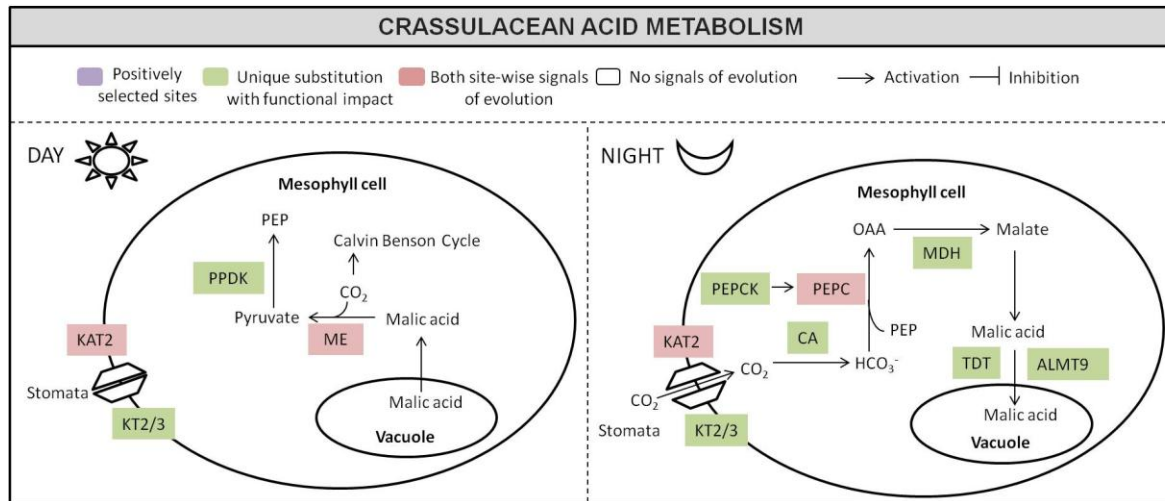
649 The values mentioned at the nodes are the bootstrap values. The scale mentioned is the nucleotide  
650 substitutions per base.

651



652  
653 **Figure 2.** The functional categories of genes that showed positive selection in *Aloe vera*

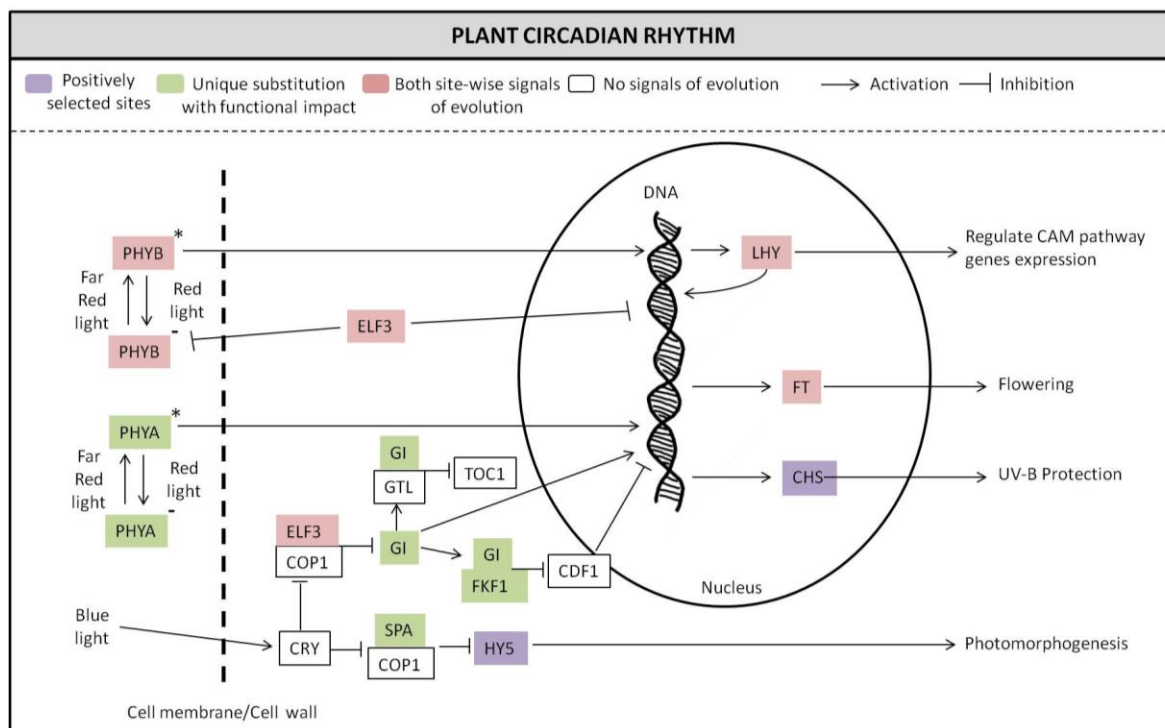
654 The standard *Arabidopsis thaliana* gene IDs were used in case of genes that did not have a standard  
655 gene symbol.



656

657 **Figure 3.** The adaptive evolution of CAM pathway in *Aloe vera*

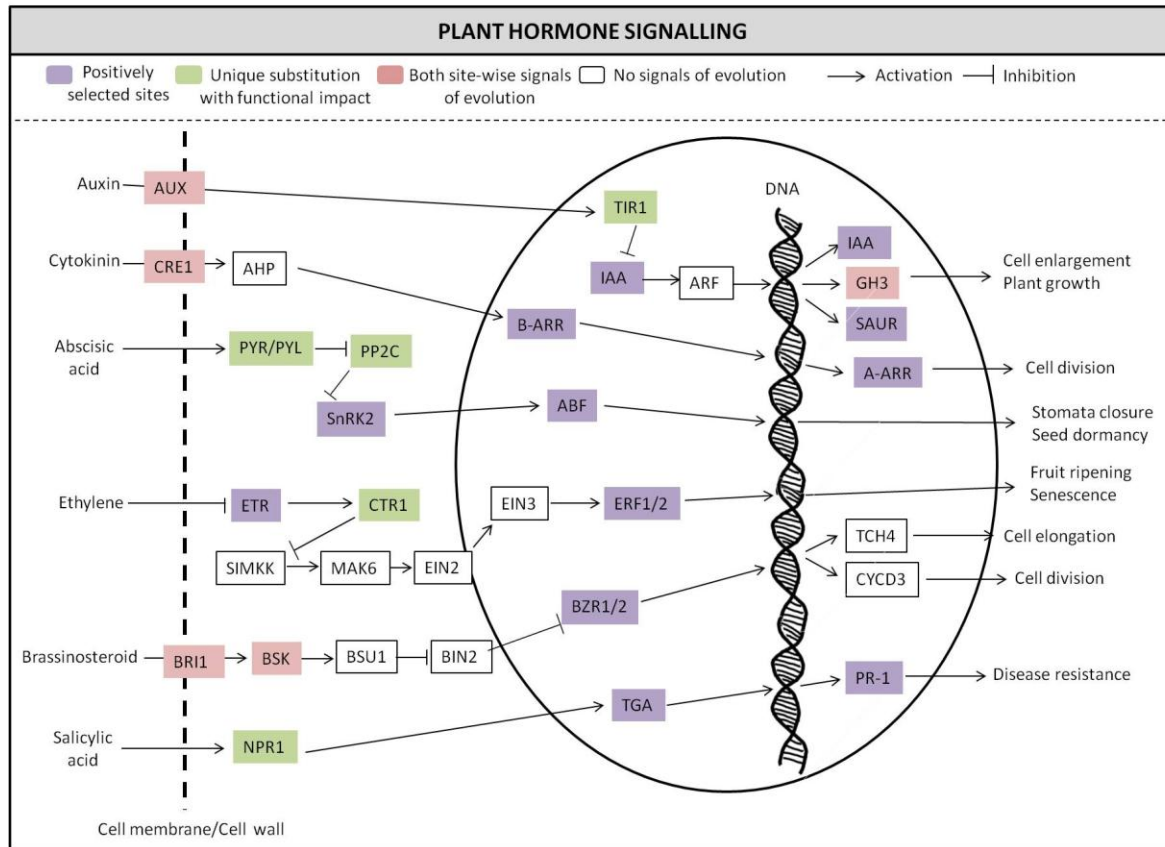
658 The important genes of the CAM pathway are shown with their function in the day time and night  
 659 time metabolism. The genes in Levander color had positively selected codon sites, the genes in  
 660 Green color had unique substitutions with function impact, and the genes in Red color showed both  
 661 the signs of site-specific adaptive evolution in *Aloe vera*. There were no CAM pathway genes that  
 662 had only positively selected codon sites.



663

664 **Figure 4.** The adaptive evolution of circadian rhythm pathway in *Aloe vera*

665 The important genes of the plant circadian rhythm are shown with their function. The genes in  
 666 Levander color had positively selected codon sites, the genes in Green color had unique  
 667 substitutions with function impact, and the genes in Red color showed both the signs of site-specific  
 668 adaptive evolution in *Aloe vera*.



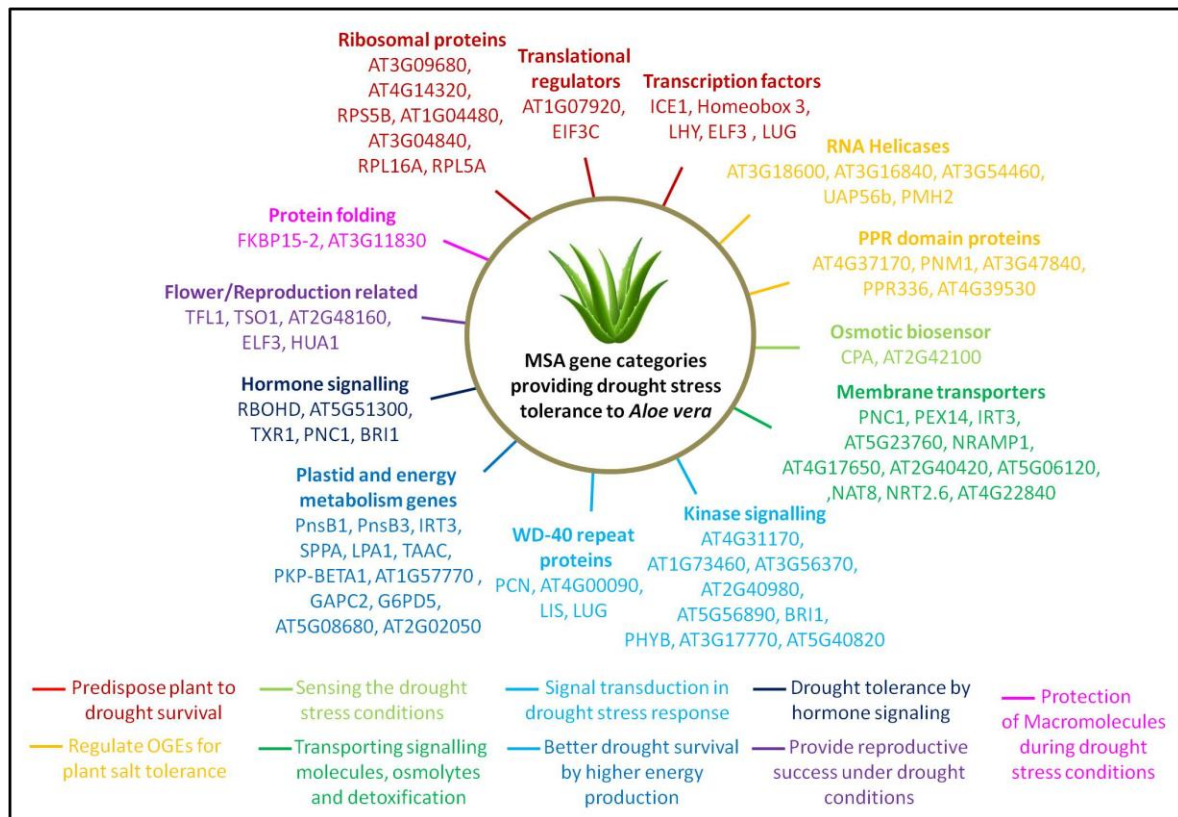
669

670 **Figure 5.** The adaptive evolution of plant hormone signaling pathway in *Aloe vera*

671 The important genes of the auxin, cytokinin, abscisic acid, ethylene, brassinosteroid, and salicylic  
 672 acid signaling pathways are shown with their function. The genes in Levander color had positively  
 673 selected codon sites, the genes in Green color had unique substitutions with function impact, and  
 674 the genes in Red color showed both the signs of site-specific adaptive evolution in *Aloe vera*.

675





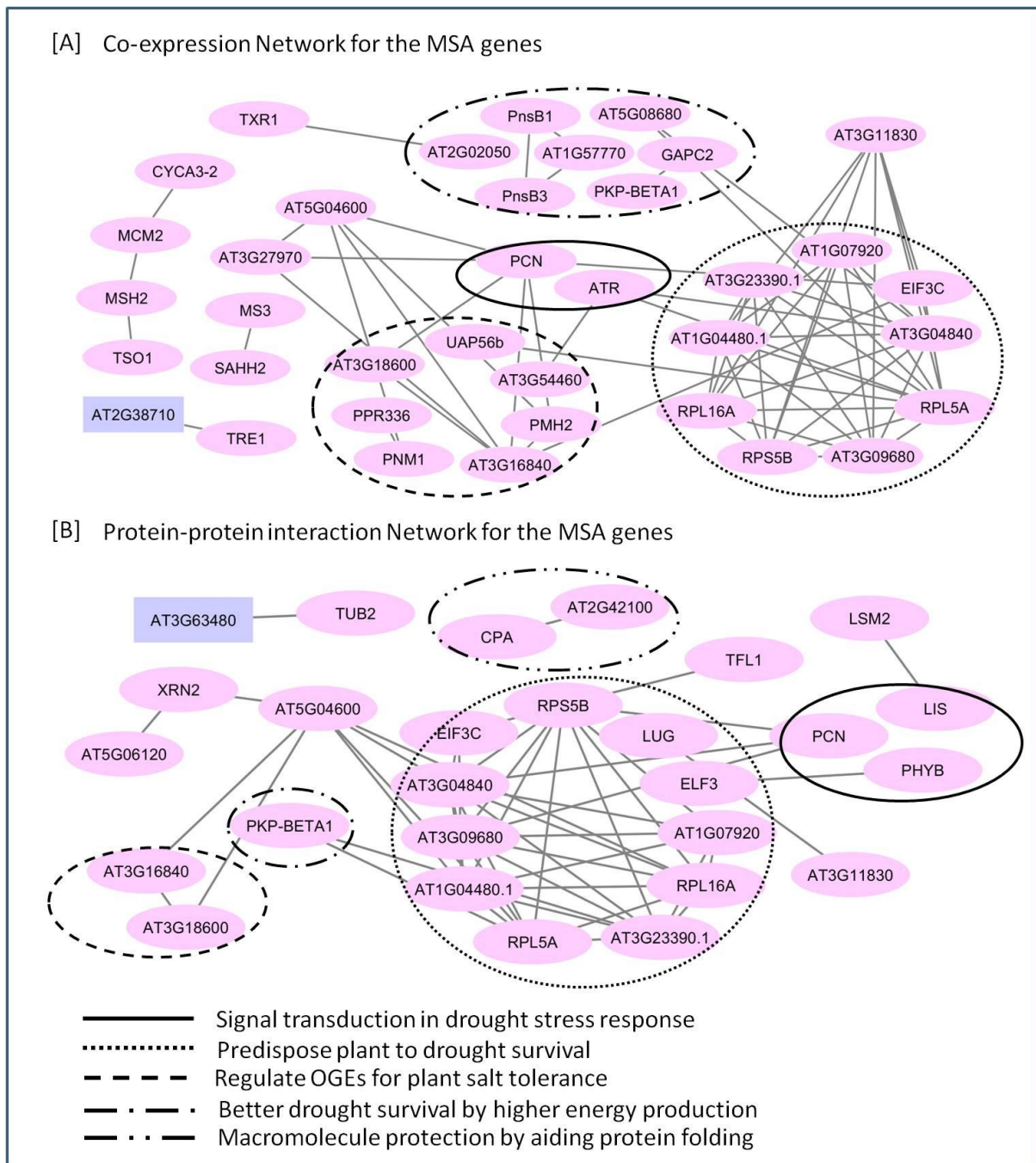
676

677 **Figure 6.** The MSA genes in *Aloe vera* that are involved in drought stress response

678 The relation of specific categories of genes with drought stress response was determined from the  
 679 literature. The standard *Arabidopsis thaliana* gene IDs were used in case of genes that did not have a  
 680 standard gene symbol.

681





682

683 **Figure 7.** Evaluating the co-expression and physical interaction of MSA genes in *Aloe vera*

684 [A] The co-expression network of the MSA genes is shown. Only the MSA genes that showed at least  
 685 one co-expression connection are shown. The nodes represent the genes, and the edges represent  
 686 the co-expression of the connected nodes.

687 [B] The protein-protein interaction network of the MSA genes is shown. Only the MSA genes that  
 688 showed at least one protein-protein interaction are shown. The nodes represent the genes, and the  
 689 edges represent the protein-protein interaction between the connected nodes.

690 Note: The standard *Arabidopsis thaliana* gene IDs were used in case of genes that did not have a  
 691 standard gene symbol.

692 REFERENCES

- 693 1. Silva H, Sagardia S, Seguel O, Torres C, Tapia C, Franck N, Cardemil L: **Effect of water**  
694 **availability on growth and water use efficiency for biomass and gel production in Aloe**  
695 **Vera (Aloe barbadensis M.).** *Industrial Crops and Products* 2010, **31**(1):20-27.
- 696 2. Grace OM, Buerki S, Symonds MR, Forest F, van Wyk AE, Smith GF, Klopper RR, Bjorå CS,  
697 Neale S, Demissew S: **Evolutionary history and leaf succulence as explanations for**  
698 **medicinal use in aloes and the global popularity of Aloe vera.** *BMC evolutionary biology*  
699 2015, **15**(1):29.
- 700 3. Reynolds T, Dweck A: **Aloe vera leaf gel: a review update.** *Journal of ethnopharmacology*  
701 1999, **68**(1-3):3-37.
- 702 4. Gupta VK, Malhotra S: **Pharmacological attribute of Aloe vera: Revalidation through**  
703 **experimental and clinical studies.** *Ayu* 2012, **33**(2):193.
- 704 5. Raksha B, Pooja S, Babu S: **Bioactive compounds and medicinal properties of Aloe vera L.:**  
705 **An update.** *Journal of Plant Sciences* 2014, **2**(3):102-107.
- 706 6. Hamman JH: **Composition and applications of Aloe vera leaf gel.** *Molecules* 2008,  
707 **13**(8):1599-1616.
- 708 7. Joseph B, Raj SJ: **Pharmacognostic and phytochemical properties of Aloe vera linn an**  
709 **overview.** *International journal of pharmaceutical sciences review and research* 2010,  
710 **4**(2):106-110.
- 711 8. Choudhri P, Rani M, Sangwan RS, Kumar R, Kumar A, Chhokar V: **De novo sequencing,**  
712 **assembly and characterisation of Aloe vera transcriptome and analysis of expression**  
713 **profiles of genes related to saponin and anthraquinone metabolism.** *BMC genomics* 2018,  
714 **19**(1):427.
- 715 9. NOBEL PS, JORDAN PW: **Transpiration stream of desert species: resistances and**  
716 **capacitances for a C3, a C4, and a CAM plant.** *Journal of experimental botany* 1983,  
717 **34**(10):1379-1391.
- 718 10. Jin ZM, Wang CH, Liu ZP, Gong WJ: **Physiological and ecological characters studies on Aloe**  
719 **vera under soil salinity and seawater irrigation.** *Process Biochemistry* 2007, **42**(4):710-714.
- 720 11. Delatorre-Herrera J, Delfino I, Salinas C, Silva H, Cardemil L: **Irrigation restriction effects on**  
721 **water use efficiency and osmotic adjustment in Aloe Vera plants (Aloe barbadensis Miller).**  
722 *Agricultural Water Management* 2010, **97**(10):1564-1570.
- 723 12. Adams SP, Leitch IJ, Bennett MD, Chase MW, Leitch AR: **Ribosomal DNA evolution and**  
724 **phylogeny in Aloe (Asphodelaceae).** *American Journal of Botany* 2000, **87**(11):1578-1583.
- 725 13. Treutlein J, Smith GF, Van Wyk B-E, Wink M: **Phylogenetic relationships in Asphodelaceae**  
726 **(subfamily Alooideae) inferred from chloroplast DNA sequences (rbcL, matK) and from**  
727 **genomic fingerprinting (ISSR).** *Taxon* 2003, **52**(2):193-207.
- 728 14. Qian H, Jin Y: **An updated megaphylogeny of plants, a tool for generating plant phylogenies**  
729 **and an analysis of phylogenetic community structure.** *Journal of Plant Ecology* 2016,  
730 **9**(2):233-239.
- 731 15. Chase MW, Christenhusz M, Fay M, Byng J, Judd WS, Soltis D, Mabberley D, Sennikov A,  
732 Soltis PS, Stevens PF: **An update of the Angiosperm Phylogeny Group classification for the**  
733 **orders and families of flowering plants: APG IV.** *Botanical Journal of the Linnean Society*  
734 2016, **181**(1):1-20.
- 735 16. Zonneveld BJ: **Genome size analysis of selected species of Aloe (Aloaceae) reveals the most**  
736 **primitive species and results in some new combinations.** *Bradleya* 2002, **2002**(20):5-12.
- 737 17. Bolger AM, Lohse M, Usadel B: **Trimmomatic: a flexible trimmer for Illumina sequence**  
738 **data.** *Bioinformatics* 2014, **30**(15):2114-2120.
- 739 18. Simpson JT, Durbin R: **Efficient de novo assembly of large genomes using compressed data**  
740 **structures.** *Genome research* 2012, **22**(3):549-556.

- 741 19. Birol I, Jackman SD, Nielsen CB, Qian JQ, Varhol R, Stazyk G, Morin RD, Zhao Y, Hirst M,  
742 Schein JE: **De novo transcriptome assembly with ABySS**. *Bioinformatics* 2009, **25**(21):2872-  
743 2877.
- 744 20. Ruan J, Li H: **Fast and accurate long-read assembly with wtdbg2**. *Nature methods* 2020,  
745 **17**(2):155-158.
- 746 21. Mittal P, Jaiswal SK, Vijay N, Saxena R, Sharma VK: **Comparative analysis of corrected tiger  
747 genome provides clues to its neuronal evolution**. *Scientific reports* 2019, **9**(1):1-11.
- 748 22. Song L, Shankar DS, Florea L: **Rascaf: improving genome assembly with RNA sequencing  
749 data**. *The plant genome* 2016, **9**(3).
- 750 23. Benson G: **Tandem repeats finder: a program to analyze DNA sequences**. *Nucleic acids  
751 research* 1999, **27**(2):573-580.
- 752 24. Bolser D, Staines DM, Pritchard E, Kersey P: **Ensembl plants: integrating tools for visualizing,  
753 mining, and analyzing plant genomics data**. In: *Plant bioinformatics*. Springer; 2016: 115-  
754 140.
- 755 25. Howe KL, Contreras-Moreira B, De Silva N, Maslen G, Akanni W, Allen J, Alvarez-Jarreta J,  
756 Barba M, Bolser DM, Cambell L: **Ensembl Genomes 2020—enabling non-vertebrate  
757 genomic research**. *Nucleic acids research* 2020, **48**(D1):D689-D695.
- 758 26. Griffiths-Jones S, Saini HK, van Dongen S, Enright AJ: **miRBase: tools for microRNA genomics**.  
759 *Nucleic acids research* 2007, **36**(suppl\_1):D154-D158.
- 760 27. Chan PP, Lowe TM: **tRNAscan-SE: searching for tRNA genes in genomic sequences**. In: *Gene  
761 Prediction*. Springer; 2019: 1-14.
- 762 28. Wickett NJ, Mirarab S, Nguyen N, Warnow T, Carpenter E, Matasci N, Ayyampalayam S,  
763 Barker MS, Burleigh JG, Gitzendanner MA: **Phylotranscriptomic analysis of the origin and  
764 early diversification of land plants**. *Proceedings of the National Academy of Sciences* 2014,  
765 **111**(45):E4859-E4868.
- 766 29. Haas BJ, Papanicolaou A, Yassour M, Grabherr M, Blood PD, Bowden J, Couger MB, Eccles D,  
767 Li B, Lieber M: **De novo transcript sequence reconstruction from RNA-seq using the Trinity  
768 platform for reference generation and analysis**. *Nature protocols* 2013, **8**(8):1494.
- 769 30. Kim D, Langmead B, Salzberg SL: **HISAT: a fast spliced aligner with low memory  
770 requirements**. *Nature methods* 2015, **12**(4):357-360.
- 771 31. Waterhouse RM, Seppey M, Simão FA, Manni M, Ioannidis P, Klioutchnikov G, Kriventseva  
772 EV, Zdobnov EM: **BUSCO applications from quality assessments to gene prediction and  
773 phylogenomics**. *Molecular biology and evolution* 2018, **35**(3):543-548.
- 774 32. Simão FA, Waterhouse RM, Ioannidis P, Kriventseva EV, Zdobnov EM: **BUSCO: assessing  
775 genome assembly and annotation completeness with single-copy orthologs**. *Bioinformatics*  
776 2015, **31**(19):3210-3212.
- 777 33. Campbell MS, Holt C, Moore B, Yandell M: **Genome annotation and curation using MAKER  
778 and MAKER-P**. *Current protocols in bioinformatics* 2014, **48**(1):4.11. 11-14.11. 39.
- 779 34. Stanke M, Keller O, Gunduz I, Hayes A, Waack S, Morgenstern B: **AUGUSTUS: ab initio  
780 prediction of alternative transcripts**. *Nucleic acids research* 2006, **34**(suppl\_2):W435-W439.
- 781 35. Stanke M, Steinkamp R, Waack S, Morgenstern B: **AUGUSTUS: a web server for gene finding  
782 in eukaryotes**. *Nucleic acids research* 2004, **32**(suppl\_2):W309-W312.
- 783 36. Altschul SF, Gish W, Miller W, Myers EW, Lipman DJ: **Basic local alignment search tool**.  
784 *Journal of molecular biology* 1990, **215**(3):403-410.
- 785 37. Suzek BE, Wang Y, Huang H, McGarvey PB, Wu CH, Consortium U: **UniRef clusters: a  
786 comprehensive and scalable alternative for improving sequence similarity searches**.  
787 *Bioinformatics* 2015, **31**(6):926-932.
- 788 38. Bateman A, Coin L, Durbin R, Finn RD, Hollich V, Griffiths-Jones S, Khanna A, Marshall M,  
789 Moxon S, Sonnhammer EL: **The Pfam protein families database**. *Nucleic acids research*  
790 2004, **32**(suppl\_1):D138-D141.

- 791 39. Finn RD, Clements J, Eddy SR: **HMMER web server: interactive sequence similarity**  
792 **searching**. *Nucleic acids research* 2011, **39**(suppl\_2):W29-W37.
- 793 40. Buchfink B, Xie C, Huson DH: **Fast and sensitive protein alignment using DIAMOND**. *Nature*  
794 *methods* 2015, **12**(1):59.
- 795 41. Fu L, Niu B, Zhu Z, Wu S, Li W: **CD-HIT: accelerated for clustering the next-generation**  
796 **sequencing data**. *Bioinformatics* 2012, **28**(23):3150-3152.
- 797 42. Zerbino DR, Achuthan P, Akanni W, Amode MR, Barrell D, Bhai J, Billis K, Cummins C, Gall A,  
798 Girón CG: **Ensembl 2018**. *Nucleic acids research* 2018, **46**(D1):D754-D761.
- 799 43. Emms DM, Kelly S: **OrthoFinder: phylogenetic orthology inference for comparative**  
800 **genomics**. *Genome biology* 2019, **20**(1):1-14.
- 801 44. Laetsch DR, Blaxter ML: **KinFin: software for Taxon-Aware analysis of clustered protein**  
802 **sequences**. *G3: Genes, Genomes, Genetics* 2017, **7**(10):3349-3357.
- 803 45. Katoh K, Standley DM: **MAFFT multiple sequence alignment software version 7:**  
804 **improvements in performance and usability**. *Molecular biology and evolution* 2013,  
805 **30**(4):772-780.
- 806 46. Stamatakis A: **RAxML version 8: a tool for phylogenetic analysis and post-analysis of large**  
807 **phylogenies**. *Bioinformatics* 2014, **30**(9):1312-1313.
- 808 47. Jombart T, Dray S, Dray MS: **Package 'adephylo'**. 2017.
- 809 48. Jombart T, Dray S: **adephylo: exploratory analyses for the phylogenetic comparative**  
810 **method**. *Bioinformatics* 2010, **26**(15):1-21.
- 811 49. Yang Z: **PAML 4: phylogenetic analysis by maximum likelihood**. *Molecular biology and*  
812 *evolution* 2007, **24**(8):1586-1591.
- 813 50. Liu K, Warnow TJ, Holder MT, Nelesen SM, Yu J, Stamatakis AP, Linder CR: **SATe-II: very fast**  
814 **and accurate simultaneous estimation of multiple sequence alignments and phylogenetic**  
815 **trees**. *Systematic biology* 2012, **61**(1):90.
- 816 51. Rice P, Longden I, Bleasby A: **EMBOSS: the European molecular biology open software**  
817 **suite**. In: Elsevier current trends; 2000.
- 818 52. Ng PC, Henikoff S: **SIFT: Predicting amino acid changes that affect protein function**. *Nucleic*  
819 *acids research* 2003, **31**(13):3812-3814.
- 820 53. Boutet E, Lieberherr D, Tognolli M, Schneider M, Bairoch A: **Uniprotkb/swiss-prot**. In: *Plant*  
821 *bioinformatics*. Springer; 2007: 89-112.
- 822 54. Huerta-Cepas J, Forslund K, Coelho LP, Szklarczyk D, Jensen LJ, Von Mering C, Bork P: **Fast**  
823 **genome-wide functional annotation through orthology assignment by eggNOG-mapper**.  
824 *Molecular biology and evolution* 2017, **34**(8):2115-2122.
- 825 55. Moriya Y, Itoh M, Okuda S, Yoshizawa AC, Kanehisa M: **KAAS: an automatic genome**  
826 **annotation and pathway reconstruction server**. *Nucleic acids research* 2007,  
827 **35**(suppl\_2):W182-W185.
- 828 56. Liao Y, Wang J, Jaehnig EJ, Shi Z, Zhang B: **WebGestalt 2019: gene set analysis toolkit with**  
829 **revamped UIs and APIs**. *Nucleic acids research* 2019, **47**(W1):W199-W205.
- 830 57. Szklarczyk D, Morris JH, Cook H, Kuhn M, Wyder S, Simonovic M, Santos A, Doncheva NT,  
831 Roth A, Bork P: **The STRING database in 2017: quality-controlled protein-protein**  
832 **association networks, made broadly accessible**. *Nucleic acids research* 2016:gkw937.
- 833 58. Shannon P, Markiel A, Ozier O, Baliga NS, Wang JT, Ramage D, Amin N, Schwikowski B,  
834 Ideker T: **Cytoscape: a software environment for integrated models of biomolecular**  
835 **interaction networks**. *Genome research* 2003, **13**(11):2498-2504.
- 836 59. Dolezel J, Bartos J, Voglmayr H, Greilhuber J: **Nuclear DNA content and genome size of trout**  
837 **and human**. *Cytometry Part A: the journal of the International Society for Analytical Cytology*  
838 2003, **51**(2):127-128; author reply 129.
- 839 60. Nystedt B, Street NR, Wetterbom A, Zuccolo A, Lin Y-C, Scofield DG, Vezzi F, Delhomme N,  
840 Giacomello S, Alexeyenko A: **The Norway spruce genome sequence and conifer genome**  
841 **evolution**. *nature* 2013, **497**(7451):579-584.



- 842 61. Neale DB, Wegrzyn JL, Stevens KA, Zimin AV, Puiu D, Crepeau MW, Cardeno C, Koriabine M,  
843 Holtz-Morris AE, Liechty JD: **Decoding the massive genome of loblolly pine using haploid**  
844 **DNA and novel assembly strategies.** *Genome biology* 2014, **15**(3):R59.
- 845 62. Stevens KA, Wegrzyn JL, Zimin A, Puiu D, Crepeau M, Cardeno C, Paul R, Gonzalez-Ibeas D,  
846 Koriabine M, Holtz-Morris AE: **Sequence of the sugar pine megagenome.** *Genetics* 2016,  
847 **204**(4):1613-1626.
- 848 63. Birol I, Raymond A, Jackman SD, Pleasance S, Coope R, Taylor GA, Yuen MMS, Keeling CI,  
849 Brand D, Vandervalk BP: **Assembling the 20 Gb white spruce (*Picea glauca*) genome from**  
850 **whole-genome shotgun sequencing data.** *Bioinformatics* 2013, **29**(12):1492-1497.
- 851 64. Dunemann F, Schrader O, Budahn H, Houben A: **Characterization of centromeric histone H3**  
852 **(CENH3) variants in cultivated and wild carrots (*Daucus sp.*).** *Plos one* 2014, **9**(6):e98504.
- 853 65. Wang L, Deng L: **GmACP expression is decreased in GmNORK knockdown transgenic**  
854 **soybean roots.** *The Crop Journal* 2016, **4**(6):509-516.
- 855 66. Silvera K, Winter K, Rodriguez BL, Albion RL, Cushman JC: **Multiple isoforms of phospho enol**  
856 **pyruvate carboxylase in the Orchidaceae (subtribe Oncidiinae): implications for the**  
857 **evolution of crassulacean acid metabolism.** *Journal of experimental botany* 2014,  
858 **65**(13):3623-3636.
- 859 67. Fei X, Hou L, Shi J, Yang T, Liu Y, Wei A: **Patterns of Drought Response of 38 WRKY**  
860 **Transcription Factors of *Zanthoxylum bungeanum* Maxim.** *International journal of*  
861 *molecular sciences* 2019, **20**(1):68.
- 862 68. Zhao Y, Cheng X, Liu X, Wu H, Bi H, Xu H: **The wheat MYB transcription factor TaMYB31 is**  
863 **involved in drought stress responses in Arabidopsis.** *Frontiers in plant science* 2018, **9**:1426.
- 864 69. Waseem M, Li Z: **Dissecting the Role of a Basic Helix-Loop-Helix Transcription Factor,**  
865 **S1bHLH22, Under Salt and Drought Stresses in Transgenic *Solanum lycopersicum* L.**  
866 *Frontiers in plant science* 2019, **10**:734.
- 867 70. Zhao C, Haigh AM, Holford P, Chen Z-H: **Roles of chloroplast retrograde signals and ion**  
868 **transport in plant drought tolerance.** *International journal of molecular sciences* 2018,  
869 **19**(4):963.
- 870 71. Yoo Y-H, Hong W-J, Jung K-H: **A Systematic view exploring the role of chloroplasts in plant**  
871 **abiotic stress responses.** *BioMed research international* 2019, **2019**.
- 872 72. Tuteja N, Mahajan S: **Calcium signaling network in plants: an overview.** *Plant signaling &*  
873 *behavior* 2007, **2**(2):79-85.
- 874 73. Takatsuji H: **Zinc-finger transcription factors in plants.** *Cellular and Molecular Life Sciences*  
875 *CMLS* 1998, **54**(6):582-596.
- 876 74. Agarwal P, Jha B: **Transcription factors in plants and ABA dependent and independent**  
877 **abiotic stress signalling.** *Biologia Plantarum* 2010, **54**(2):201-212.
- 878 75. Roldán-Arjona T, Ariza RR: **Repair and tolerance of oxidative DNA damage in plants.**  
879 *Mutation Research/Reviews in Mutation Research* 2009, **681**(2-3):169-179.
- 880 76. Naik PM, Al-Khayri JM: **Abiotic and biotic elicitors—role in secondary metabolites**  
881 **production through in vitro culture of medicinal plants.** *Abiotic and biotic stress in plants-*  
882 *recent advances and future perspectives* 2016:247-277.
- 883 77. Yang Y, Wang W, Chu Z, Zhu J-K, Zhang H: **Roles of nuclear pores and nucleo-cytoplasmic**  
884 **trafficking in plant stress responses.** *Frontiers in plant science* 2017, **8**:574.
- 885 78. Nisa M-U, Huang Y, Benhamed M, Raynaud C: **The plant DNA damage response: Signaling**  
886 **pathways leading to growth inhibition and putative role in response to stress conditions.**  
887 *Frontiers in plant science* 2019, **10**.
- 888 79. Arasimowicz M, Floryszak-Wieczorek J: **Nitric oxide as a bioactive signalling molecule in**  
889 **plant stress responses.** *Plant science* 2007, **172**(5):876-887.
- 890 80. Liu Y, Wu R, Wan Q, Xie G, Bi Y: **Glucose-6-phosphate dehydrogenase plays a pivotal role in**  
891 **nitric oxide-involved defense against oxidative stress under salt stress in red kidney bean**  
892 **roots.** *Plant and Cell Physiology* 2007, **48**(3):511-522.

- 893 81. Bray EA: **Molecular responses to water deficit**. *Plant physiology* 1993, **103**(4):1035.
- 894 82. Feng R-J, Ren M-Y, Lu L-F, Peng M, Guan X, Zhou D-B, Zhang M-Y, Qi D-F, Li K, Tang W:  
895 **Involvement of abscisic acid-responsive element-binding factors in cassava (*Manihot***  
896 **esculenta) dehydration stress response**. *Scientific reports* 2019, **9**(1):1-12.
- 897 83. Yamaguchi-Shinozaki K, Shinozaki K: **Transcriptional regulatory networks in cellular**  
898 **responses and tolerance to dehydration and cold stresses**. *Annu Rev Plant Biol* 2006,  
899 **57**:781-803.
- 900 84. Van Houtte H, Vandesteene L, López-Galvis L, Lemmens L, Kissel E, Carpentier S, Feil R,  
901 Avonce N, Beeckman T, Lunn JE: **Overexpression of the trehalase gene AtTRE1 leads to**  
902 **increased drought stress tolerance in Arabidopsis and is involved in abscisic acid-induced**  
903 **stomatal closure**. *Plant physiology* 2013, **161**(3):1158-1171.
- 904 85. Teeri J, Tonsor S, Turner M: **Leaf thickness and carbon isotope composition in the**  
905 **Crassulaceae**. *Oecologia* 1981, **50**(3):367-369.
- 906 86. Mallona I, Egea-Cortines M, Weiss J: **Conserved and divergent rhythms of crassulacean acid**  
907 **metabolism-related and core clock gene expression in the cactus *Opuntia ficus-indica***.  
908 *Plant physiology* 2011, **156**(4):1978-1989.
- 909 87. Silvera K, Neubig KM, Whitten WM, Williams NH, Winter K, Cushman JC: **Evolution along the**  
910 **crassulacean acid metabolism continuum**. *Functional Plant Biology* 2010, **37**(11):995-1010.
- 911 88. Santner A, Estelle M: **Recent advances and emerging trends in plant hormone signalling**.  
912 *nature* 2009, **459**(7250):1071-1078.
- 913 89. Cao Y, Luo Q, Tian Y, Meng F: **Physiological and proteomic analyses of the drought stress**  
914 **response in *Amygdalus Mira* (Koehne) Yü et Lu roots**. *BMC plant biology* 2017, **17**(1):53.
- 915 90. Janiak A, Kwasniewski M, Sowa M, Gajek K, Żmuda K, Kościelniak J, Szarejko I: **No time to**  
916 **waste: Transcriptome study reveals that drought tolerance in barley may be attributed to**  
917 **stressed-like expression patterns that exist before the occurrence of stress**. *Frontiers in*  
918 *plant science* 2018, **8**:2212.
- 919 91. Robles P, Quesada V: **Transcriptional and post-transcriptional regulation of organellar gene**  
920 **expression (OGE) and its roles in plant salt tolerance**. *International journal of molecular*  
921 *sciences* 2019, **20**(5):1056.
- 922 92. Leister D, Wang L, Kleine T: **Organellar gene expression and acclimation of plants to**  
923 **environmental stress**. *Frontiers in plant science* 2017, **8**:387.
- 924 93. Iqbal MJ: **Role of osmolytes and antioxidant enzymes for drought tolerance in wheat**.  
925 *Global Wheat Production* 2018:51.
- 926 94. Jarzyniak KM, Jasiński M: **Membrane transporters and drought resistance—a complex issue**.  
927 *Frontiers in plant science* 2014, **5**:687.
- 928 95. Ranjan A, Sawant S: **Genome-wide transcriptomic comparison of cotton (*Gossypium***  
929 **herbaceum) leaf and root under drought stress**. *3 Biotech* 2015, **5**(4):585-596.
- 930 96. Liu WC, Li YH, Yuan HM, Zhang BL, Zhai S, Lu YT: **WD40-REPEAT 5a functions in drought**  
931 **stress tolerance by regulating nitric oxide accumulation in Arabidopsis**. *Plant, cell &*  
932 *environment* 2017, **40**(4):543-552.
- 933 97. Feyissa BA, Arshad M, Gruber MY, Kohalmi SE, Hannoufa A: **The interplay between**  
934 **miR156/SPL13 and DFR/WD40-1 regulate drought tolerance in alfalfa**. *BMC plant biology*  
935 2019, **19**(1):1-19.
- 936 98. Tian F, Gong J, Zhang J, Zhang M, Wang G, Li A, Wang W: **Enhanced stability of thylakoid**  
937 **membrane proteins and antioxidant competence contribute to drought stress resistance in**  
938 **the tasg1 wheat stay-green mutant**. *Journal of experimental botany* 2013, **64**(6):1509-1520.
- 939 99. Shinozaki K, Yamaguchi-Shinozaki K: **Gene networks involved in drought stress response**  
940 **and tolerance**. *Journal of experimental botany* 2007, **58**(2):221-227.
- 941 100. Tiwari S, Lata C, Singh Chauhan P, Prasad V, Prasad M: **A functional genomic perspective on**  
942 **drought signalling and its crosstalk with phytohormone-mediated signalling pathways in**  
943 **plants**. *Current genomics* 2017, **18**(6):469-482.

- 944 101. Monroe JG, Powell T, Price N, Mullen JL, Howard A, Evans K, Lovell JT, McKay JK: **Drought**  
945 **adaptation in Arabidopsis thaliana by extensive genetic loss-of-function.** *Elife* 2018,  
946 **7:e41038.**
- 947 102. Song K, Kim HC, Shin S, Kim K-H, Moon J-C, Kim JY, Lee B-M: **Transcriptome analysis of**  
948 **flowering time genes under drought stress in maize leaves.** *Frontiers in plant science* 2017,  
949 **8:267.**
- 950 103. Huerta C, Freire M, Cardemil L: **Expression of hsp70, hsp100 and ubiquitin in Aloe**  
951 **barbadensis Miller under direct heat stress and under temperature acclimation conditions.**  
952 *Plant cell reports* 2013, **32(2):293-307.**
- 953 104. Hazrati S, Tahmasebi-Sarvestani Z, Mokhtassi-Bidgoli A, Modarres-Sanavy SAM, Mohammadi  
954 H, Nicola S: **Effects of zeolite and water stress on growth, yield and chemical compositions**  
955 **of Aloe vera L.** *Agricultural Water Management* 2017, **181:66-72.**
- 956 105. Ming R, VanBuren R, Wai CM, Tang H, Schatz MC, Bowers JE, Lyons E, Wang M-L, Chen J,  
957 Biggers E: **The pineapple genome and the evolution of CAM photosynthesis.** *Nature*  
958 *genetics* 2015, **47(12):1435-1442.**
- 959 106. Yin H, Guo H-B, Weston DJ, Borland AM, Ranjan P, Abraham PE, Jawdy SS, Wachira J, Tuskan  
960 GA, Tschaplinski TJ: **Diel rewiring and positive selection of ancient plant proteins enabled**  
961 **evolution of CAM photosynthesis in Agave.** *BMC genomics* 2018, **19(1):588.**
- 962 107. Hartwell J: **The circadian clock in CAM plants.** *Annual Plant Reviews online* 2018:211-236.

963

964